AFRL-ML-WP-TP-2007-480

NANOCOMPOSITES DERIVED FROM CARBON NANOFIBERS AND A HYPERBRANCHED POLY(ETHER-KETONE): IN SITU POLYMERIZATION, CHAIN-END MODIFICATION, AND PROPERTIES (PREPRINT)

David H. Wang, Peter Mirau, Loon-Seng Tan, Bing Li, Christopher Y. Li, and Jong-Beom Baek

MAY 2007

MATERIALS AND MANUFACTURING DIRECTORATE
AIR FORCE RESEARCH LABORATORY
AIR FORCE MATERIEL COMMAND
WRIGHT-PATTERSON AIR FORCE BASE, OH 45433-7750

REPORT DOCUMENTATION PAGE

Form Approved
OMB No. 0704-0188

1. REPORT DATE *(DD-MM-YY)*	2. REPORT TYPE	3. DATES COVERED *(From - To)*
May 2007	Journal Article Preprint	N/A

4. TITLE AND SUBTITLE

NANOCOMPOSITES DERIVED FROM CARBON NANOFIBERS AND A HYPERBRANCHED POLY(ETHER-KETONE): IN SITU POLYMERIZATION, CHAIN-END MODIFICATION, AND PROPERTIES (PREPRINT)

5a. CONTRACT NUMBER
F33615-00-D-5008

5b. GRANT NUMBER

5c. PROGRAM ELEMENT NUMBER
62102F

6. AUTHOR(S)

David H. Wang (University of Dayton Research Institute)
Peter Mirau and Loon-Seng Tan (AFRL/MLBP)
Bing Li and Christopher Y. Li (Drexel University)
Jong-Beom Baek (Chungbuk National University)

5d. PROJECT NUMBER
4347

5e. TASK NUMBER
10

5f. WORK UNIT NUMBER
FK

7. PERFORMING ORGANIZATION NAME(S) AND ADDRESS(ES)

University of Dayton Research Institute
300 College Park Avenue
Dayton, OH 45469

Polymer Branch (AFRL/MLBP)
Nonmetallic Materials Division
Materials and Manufacturing Directorate
Air Force Research Laboratory, Air Force Materiel Command
Wright-Patterson Air Force Base, OH 45433-7750

Drexel University
Department of Materials Science and Engineering
Philadelphia, PA 19104

Chungbuk National University
Dept. of Industrial Chemistry
Cheongju, Chungbuk 361-763
South Korea

8. PERFORMING ORGANIZATION REPORT NUMBER

9. SPONSORING/MONITORING AGENCY NAME(S) AND ADDRESS(ES)

Materials and Manufacturing Directorate
Air Force Research Laboratory
Air Force Materiel Command
Wright-Patterson AFB, OH 45433-7750

10. SPONSORING/MONITORING AGENCY ACRONYM(S)
AFRL-ML-WP

11. SPONSORING/MONITORING AGENCY REPORT NUMBER(S)
AFRL-ML-WP-TP-2007-480

12. DISTRIBUTION/AVAILABILITY STATEMENT
Approved for public release; distribution unlimited.

13. SUPPLEMENTARY NOTES
Journal article submitted to Chemistry of Materials. The U.S. Government is joint author of this work and has the right to use, modify, reproduce, release, perform, display, or disclose the work. PAO Case Number: AFRL/WS 07-1335, 05 Jun 2007. Paper contains color content.

14. ABSTRACT

5-Phenoxyisophthalic acid, an A_2B monomer, was easily polymerized via a Friedel-Crafts acylation in poly(phosphoric acid)/phosphorus pentoxide (PPA/P_2O_5; 1:4 w/w) medium to form a CO_2H-terminated hyperbranched poly(ether-ketone), HPB-PEK. Thus, the polymerization of 5-phenoxyisophthalic acid, in the presence of various amounts (1, 2, 5, 10, 20, 30 and 40 wt%) of vapor-grown carbon nanofibers (VGCNF) was performed under similar reaction conditions. The resulting (HPB-PEK)-*g*-VGCNF nanocomposites were insoluble in dichlorobenzene or toluene, but showed greatly improved solubility in polar solvents such as NMP, DMF, DMAc, ethanol, and even higher solubility in ethanol/triethylamine mixture or in aqueous ammonia solution, apparently stemming from the ionization of the numerous peripheral CO_2H groups. This is in contrast to our previous result that the nanocomposites derived from VGCNF similarly

Abstract continued on reverse side

15. SUBJECT TERMS
in situ, polymerization, vapor-grown carbon nanofibers (VGCNF), nanocomposites

16. SECURITY CLASSIFICATION OF:			17. LIMITATION OF ABSTRACT:	18. NUMBER OF PAGES	19a. NAME OF RESPONSIBLE PERSON (Monitor)
a. REPORT	b. ABSTRACT	c. THIS PAGE			Loon-Seng Tan
Unclassified	Unclassified	Unclassified	SAR	44	19b. TELEPHONE NUMBER *(Include Area Code)* N/A

Standard Form 298 (Rev. 8-98)
Prescribed by ANSI Std. Z39-18

14. ABSTRACT

grafted with a linear meta-poly(ether-ketone), *m*PEK, with 1-30 wt% VGCNF content had much lower solubility in these polar solvents but are more soluble in methanesulfonic acid. As a way to determine both the ease in perfoming chemical transformation on the periphery of the hyperbranched component of the resulting (HPB-PEK)-g-VGCNF nanocomposites and the endgroup effect on some of their physical properties, the 10wt% (HPB-PEK)-g-VGCNF bearing carboxylic-acid endgroups were converted to benzothiazole, dodecyl ester and amine endgroups. For example, the dodecyl-terminated nanocomposite displayed an excellent solubility in chloroform and a much lower T_g than the CO_2H-terminated analog. The overall evidence based on the data from elemental analysis, thermogravimetric analysis (TGA), Fourier-transform infrared spectroscopy (FT-IR), nuclear magnetic resonance (NMR), scanning electron microscopy (SEM) as well as transmission electron microscopy (TEM) of the resulting materials implicates that under our reaction conditions, HPB-PEK was grafted to the surfaces of VGCNF resulting in the formation of highly coated nanofibers. TGA, SEM and TEM data also support that VGCNF has remained more or less structurally intact under the mildly acidic, relatively high-shearing and hot polymerization conditions.

TOC Graphic and Summary

David H. Wang, Peter Mirau, Bing Li, Christopher Y. Li, Jong-Beom Baek, and Loon-Seng Tan*

Chem. Mater. **2007**, *xx*. xxxx

Nanocomposites derived from Carbon Nanofibers and a Hyperbranched Poly(ether-ketone):: *In-situ* Polymerization, Chain-end Modification & Properties

Friedel-Crafts polymerization of 5-phenoxyisophthalic acid (AB_2 monomer), in the presence of various amounts (1, 2, 5, 10, 20, 30 and 40 wt%) of vapor-grown carbon nanofibers (VGCNF) was conducted. The terminal CO_2H-groups of hyperbranched PEK were modified with various functionalities. Our results provide some insights into controlling solubility/nano-dispersibility and thermal properties of high CNF-content polymer nanocomposites.

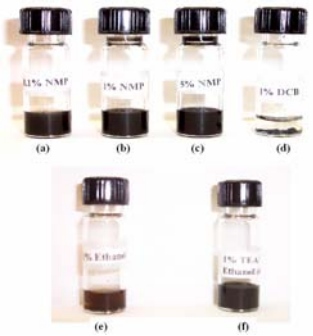

Abstract

5-Phenoxyisophthalic acid, an A_2B monomer, was easily polymerized via a Friedel-Crafts acylation in poly(phosphoric acid)/phosphorus pentoxide (PPA/P_2O_5; 1:4 w/w) medium to form a CO_2H-terminated hyperbranched poly(ether-ketone), HPB-PEK. Thus, the polymerization of 5-phenoxyisophthalic acid, in the presence of various amounts (1, 2, 5, 10, 20, 30 and 40 wt%) of vapor-grown carbon nanofibers (VGCNF) was performed under similar reaction conditions. The resulting (HPB-PEK)-*g*-VGCNF nanocomposites were insoluble in dichlorobenzene or toluene, but showed greatly improved solubility in polar solvents such as NMP, DMF, DMAc, ethanol, and even higher solubility in ethanol/triethylamine mixture or in aqueous ammonia solution, apparently stemming from the ionization of the numerous peripheral CO_2H groups. This is in contrast to our previous result that the nanocomposites derived from VGCNF similarly grafted with a linear meta-poly(ether-ketone), *m*PEK, with 1-30 wt% VGCNF content had much lower solubility in these polar solvents but are more soluble in methanesulfonic acid. As a way to determine both the ease in perfoming chemical transformation on the periphery of the hyperbranched component of the resulting (HPB-PEK)-g-VGCNF nanocomposites and the endgroup effect on some of their physical properties, the 10wt% (HPB-PEK)-g-VGCNF bearing carboxylic-acid endgroups were converted to benzothiazole, dodecyl ester and amine endgroups. For example, the dodecyl-terminated nanocomposite displayed an excellent solubility in chloroform and a much lower T_g than the CO_2H-terminated analog. The overall evidence based on the data from elemental analysis, thermogravimetric analysis (TGA), Fourier-transform infrared spectroscopy (FT-IR), nuclear magnetic resonance (NMR), scanning electron microscopy (SEM) as well as transmission electron microscopy (TEM) of the resulting materials implicates that under our reaction conditions, HPB-PEK was grafted to the surfaces of VGCNF resulting in the formation of highly coated nanofibers. TGA, SEM and TEM data also support that VGCNF has remained more or less structurally intact under the mildly acidic, relatively high-shearing and hot polymerization conditions.

Introduction

Carbon nanotubes (CNTs) such as single-walled (SWNT) and multiwalled (MWNT) nanotubes,[1] and more recently, double-walled (DWNT),[2] and few-walled (FWNT)[3] have sparked an unabated excitement in materials research because of the technological opportunities that their thermal, electrical, mechanical, and optical properties could offer. They are being actively investigated with respect to their structural reinforcement, energy/electron transport or storage capabilities, and interactions with electromagnetic waves as well as the efficient ways to transfer their outstanding properties to the polymeric matrices. A common goal is that the resulting polymer nanocomposites would be attractive in various advanced applications, where affordability, light-weight and multifunctionality are specified. However, in comparison to CNTs, vapor-grown carbon nanofibers (VGCNF), which are structurally hollow and multi-walled, but 1-2 orders of magnitude larger in diameter than MWNT and SWNT, are more practical in terms of their relatively low cost and availability in greater quantities as the result of their more advanced stage in commercial production.[4,5,6] These carbon nanofibers are typically produced by a vapor-phase catalytic process in which a carbon-containing feedstock (e.g. CH_4, C_2H_2, C_2H_4 etc.) is pyrolyzed in the presence of small metal catalyst (e.g. ferrocene, $Fe(CO)_5$ etc.) and have an outer diameter of 60-200 nm, a hollow core of 30-90 nm, and length on the order of 50-100 microns.[7,8] It follows that having aspect ratios (length/diameter) of greater than 800 should make them useful as nano-level reinforcement for polymeric matrices. Furthermore, since their inherent electrical and thermal transport properties are also excellent, there are many innovative possibilities for tailoring their polymer matrix composites into cost-effective, multifunctional materials. We have also rationalized that the similarity in the chemical and structural features between carbon nanofibers and multi-walled nanotubes, *viz.* the structural defects, should allow an easy translation of synthetic tools and scale-up processes developed for VGCNF to more expensive DWNT, FWNT or MWNT. This indeed has been found to be the case for a numbers of instances in our research efforts.

In the wake of our success in greatly improving the effectiveness of Friedel-Crafts acylation reaction in an optimized mixture of poly(phosphoric acid) and phosphorus pentoxide (PPA/P_2O_5) in poly(ether-ketone) or PEK synthesis,[9] we then extended its application to effect surface modifications of carbon nanofiber (CNF) and MWNT with carbonyl-based aromatic moieties as well as linear PEKs.[10] Apart from being an efficient Friedel-Crafts catalyst, the

PPA/P_2O_5 medium is moderately acidic but effective enough to promote homogeneous dispersion of CNF and MWNT at relatively low temperature, avoiding the premature onset of Friedel-Crafts reaction, and its relatively high viscosity impedes reaggregation of CNF and MWNT. As a result, a uniform grafting of linear PEK's onto CNF and MWNT has been achieved. However, these nanocomposites were found to be more soluble in strong acids than in common organic solvents. This finding has prodded us to explore the use of "aromatic hyperbranched polymer" approach to improving the solubilization of carbon nanofibers and nanotubes. This is because solubility (or nano-dispersibility) in organic and aqueous solvents is an important pre-requisite to the processing and fabrication of these nanocomposites on large surface areas. Furthermore, the non-entangling nature of hyperbranched structures should also aid in controlling the solution or melt viscosity during the processing of the resulting of the resulting nanocomposites .

Various in-situ polymerization methods in grafting hyperbranched polymers to or from the surfaces of carbon nanofibers[11] and carbon nanotubes have been reported in the litereature: (a) transfer radical polymerization (ATRP);[12] (b) ring-opening polymerization;[13] (c) self-condensing vinyl polymerization (SCPV);[14] (d) polycondensation.[15] In a recent example, SWNT was grafted with poly(aminoamine) dendrimers using a divergent methodology.[16] In all cases, (a) the CNF/CNT surfaces were prefunctionalized with appropriate functional groups for the subsequent polymerization processes; (b) either aliphatic or partially aliphatic hyperbranched polymers were resulted. In our case, no such prefunctionalization was required, and the resulting hyperbranched poly(ether-ketone) is wholly aromatic. We have reported the initial results of this effort,[17] and herein, we present a more comprehensive account of our investigation.

Experimental Section

Materials: All reagents and solvents were purchased from Aldrich Chemical Inc. and used as received, unless otherwise specified. Vapor-grown carbon nanofibers (VGCNF, PR-19-HT) were obtained from Applied Science Inc. (ASI), Cedarville, OH, USA via an Air Force contract

Instrumentation. Proton and carbon nuclear magnetic resonance (^{1}H-NMR and ^{13}C-NMR) spectra for intermediates and A_2B monomer were measured at 270 and 50 MHz on a Jeol-270 spectrometer. Proton nuclear magnetic resonance spectra of polymer composites were

measured at 300 MHz on a Bruker AVANCE 300 spectrometer. Infrared (IR) spectra were recorded on a Nicolet Nexus 470 Fourier transform spectrophotometer. Elemental analysis and mass spectral analysis were performed by System Support Branch, Materials Directorate, Air Force Research Lab, Dayton, Ohio. The melting points (m.p.) of all compounds were determined on a Mel-Temp melting point apparatus and are uncorrected. Intrinsic viscosities were determined with Cannon-Ubbelohde No. 75 viscometer. Flow times were recorded for *N*-methyl-2-pyrrolidinone (NMP) solution with 1 wt% lithium bromide and polymer concentrations of approximately 0.5-0.10 g/dL at 30.0 ± 0.1°C. Differential scanning calorimetry (DSC) analysis were performed in nitrogen with a heating rate of 10°C/min using a Perkin-Elmer model 2000 thermal analyzer equipped with differential scanning calorimetry cell. Themogravimetric analysis (TGA) was conducted in nitrogen (N_2) and air atmospheres at a heating rate of 10°C/min using a TA Hi-Res TGA 2950 themogravimetric analyzer. The scanning electron microscope (SEM) used in this work was a Hitachi S-5200. TEM experiments were conducted using a JEOL-2000FX microscope with an accelerating voltage of 120 kV. Sonication was conducted at 20 kHz with a 600W-power using Ace Glass GEX 600-5 Ultrsonic Processor.

The A_2B monomer (**2**, where A denoted acid function and B, aromatic C-H), 5-phenoxyisophthalic acid,[18] was synthesized in a two-step sequence, following slightly modified literature procedures:

1,3-Dimethyl-5-phenoxybenzene.[18,19] Into a 250 mL three-necked, round-bottomed flask equipped with a magnetic stir-bar, nitrogen inlet and a Dean-Stark trap, phenol (61.0 g, 0.648 mol), toluene (60 mL) and KOH (30.3g, 0.540 mol) were charged and heated at 145 °C for 3 h with water collected in the Dean-Stark trap. Then, excess phenol and water were removed under reduced pressure at 160 °C for 3 h. Copper (1.0 g), 5-bromo-m-xylene (20.0 g, 0.108 mol) and phenol (30 mL) were added to the dry salt. The mixture was agitated under dry nitrogen at 220 °C for 3 h. The reaction mixture was poured slowly into water (2000 mL) and 5wt% NaOH solution was added to dissolve excess phenol. The mixture was extracted with ethyl acetate (3 x 700 mL). The combined extract was dried and evaporated to dryness. The product was further purified by column chromatography (eluent CH_2Cl_2/hexane 1:7) to afford 19.9 g (93%) of a colorless liquid. Anal. Calcd. for $C_{14}H_{14}O$: C, 84.81%; H, 7.12%. Found: C, 84.59%; H, 7.39%. FT-IR (KBr, cm^{-1}): 3039, 2918, 1614, 1585, 1490, 1299, 1220, 1163, 1136, 1027, 950,

850, 756. Mass spectrum (m/e): 198 (M^+, 100% relative abundance). ^{1}H-NMR ($CDCl_3$, δ in ppm): 2.25 (s, 6H), 6.62 (s, 2H), 6.71 (s, 1H), 6.96 (d, 2H), 7.04 (t, 1H), 7.28 (dd, 2H). ^{13}C-NMR ($CDCl_3$, δ in ppm): 21.25, 116.60, 118.79, 122.91, 124.95, 129.62, 139.49, 157.12, 157.41.

5-Phenoxyisophthalic acid,[18,20] (**2**). Into a 1-L three-necked, round-bottomed flask equipped with a magnetic stir-bar, nitrogen inlet and a condenser, 1,3-dimethyl-5-phenoxybenzene (18.0 g, 90.8 mmol), water (140 mL) and pyridine (350 mL) were placed and heated to 100 °C. Potassium permanganate (160 g, 1.02 mol) were added in small portions over a 6-hour period. Then the mixture was agitated at 120 °C for 36 h. The manganese dioxide was removed by filtration and washed several time with hot water. The combined filtrate was acidified with dilute HCl solution. The product was collected by filtration and recrystallized from acetic acid to afford 18.0 g (77%) of white crystals, m.p. 301-303 °C (Lit. melting point not reported). Anal. Calcd. for $C_{14}H_{10}O_5$: C, 65.12%; H, 3.90%. Found: C, 64.93%; H, 4.09%. FT-IR (KBr, cm^{-1}): 3421, 2826 (Broad, COOH), 2568, 1690(C=O), 1586, 1491, 1320, 1281, 1202, 974, 757. Mass spectrum (m/e): 258 (M^+, 100% relative abundance). ^{1}H-NMR ($CDCl_3$+DMSO-d_6, δ in ppm): 7.05 (d, 2H), 7.17 (t, 1H), 7.39 (dd, 2H), 7.80 (d, 2H), 8.40 (t, 1H), 8.82 (br. s, 2H). ^{13}C-NMR ($CDCl_3$+DMSO-d_6, δ in ppm): 119.22, 123.14, 124.09, 125.38, 129.99, 133.01, 156.05, 157.46, 166.85.

Representative Procedure for *In-situ* Polymerization (HBP-PEK with 10 wt% VGCNF, 3e): Into a 250 mL resin flask equipped with a high torque mechanical stirrer, and nitrogen inlet and outlet, 5-phenoxyisophthalic acid (1.80 g, 6.98 mmol), VGCNF (0.20 g) and PPA (83% P_2O_5 assay, 40 g) were charged and stirred with dried nitrogen purging at 130 °C for 4 h. Phosphorus pentoxide (P_2O_5, 10 g) was added in one portion. The initially dark mixture became lighter and more viscous as the functionalization of VGCNF progressed. After 12 h at 130 °C, the reaction mixture was so viscous that it started to stick to the stirring rod. The temperature was maintained at 130 °C for 48 h. At the end of the reaction water was added into the flask. The resulting black polymer clusters were put into a Waring blender and the polymer bundles were chopped, collected by suction filtration, and Soxhlet- extracted with water for three days and methanol for three more days. It was then dried over P_2O_5 under reduced pressure at 120 °C for 72 h to give the product in quantitative yield. Anal. Calcd. for $C_{16.39}H_8O_4$: C, 73.22%;

H, 2.98%; O, 23.81%. Found: C, 72.94%; H, 3.12%; O, 21.74%. FT-IR (KBr, cm^{-1}): 3425, 3071, 1721 (COOH), 1659 (C=O), 1584, 1501, 1413, 1237, 1163, 760.

PPA-treated VGCNF: PPA-treated VGCNF was prepared from VGCNF (0.50 g), PPA (83% P_2O_5 assay, 20 g) and phosphorus pentoxide (P_2O_5, 5.0 g) following the same procedure used for the synthesis of **(HBP-PEK)-g-VGCNF, 3e,** to afford 0.47 (94% yield based on initial amount) of a black solid. Found: C, 98.66%; H, 0.93%; N, <0.20%; O, <0.10%.

Benzothiazole-terminated (HBP-PEK)-g-VGCNF (**4**): Into a 250 mL resin flask equipped with a high torque mechanical stirrer, and nitrogen inlet and outlet, **(HBP-PEK)-g-VGCNF, 3e** (4.0 g, 10.1 mmol), 2-aminothiophenol (3.5 g, 28.0 mmol), phosphorus pentoxide (P_2O_5, 20 g) and PPA (83% P_2O_5 assay, 80 g) were charged and stirred with dry nitrogen purging at 150 °C for 24 h. At the end of the reaction water was added into the flask. The resulting black polymeric clusters were put into a Waring blender and the polymer bundles were chopped, collected by suction filtration, and Soxhlet extracted with water for three days and methanol for three days. It was then dried over P_2O_5 under reduced pressure at 120°C for 72 h to give the product in quantitative yield. Anal. Calcd. for $C_{22.39}H_{11}NO_3S$: C, 71.92%; H, 2.94%; N, 3.74%; O, 12.84%. Found: C, 72.44%; H, 3.55%; N, 3.98%; O, 12.53%. FT-IR (KBr, cm^{-1}): 3452, 3057, 1660 (C=O), 1604, 1581, 1500, 1311, 1222, 1166, 757.

Dodecyl-terminated (HBP-PEK)-g-VGCNF (**5**): Into a 100 mL three necked flask equipped with a mechanical stirrer, and nitrogen inlet and outlet, **(HBP-PEK)-g-VGCNF, 3e** (2.0 g, 5.04 mmol), 1-dodecanol (4.0 g, 21.4 mmol), N,N'-dicyclohexylcarbodiimide (DCC, 2.10 g, 10.2 mmol), 4-(N'N-dimethylamino)pyridine (DMAP, 0.2 g) and N,N-dimethylformamide (200 mL) were charged and stirred with dried nitrogen purging at room temperature for 3 d. At the end of the reaction it was poured into water. The resulting black polymeric material collected by suction filtration and Soxhlet-extracted with methanol for more three days. It was then dried over P_2O_5 under reduced pressure at 120°C for 72 h to give the product in quantitative yield. Anal. Calcd. for $C_{28.39}H_{32}O_4$: C, 78.67%; H, 7.32%; O, 13.93%. Found: C, 79.66%; H, 7.76%; O, 14.65%. FT-IR (KBr, cm^{-1}): 2925, 2854, 1723 (ester), 1660 (C=O), 1582, 1232, 1163, 1002, 991.

Amine-terminated (HBP-PEK)-g-VGCNF (**6**): Into a 100 mL resin flask equipped with a high torque mechanical stirrer and nitrogen inlet and outlet, compound **(HBP-PEK)-g-VGCNF, 3e** (1.0 g, 2.52 mmol) and methanesulfonic acid (MSA, 16.7 g) were charged and stirred with dry nitrogen purging at room temperature. Sodium azide (0.19 g, 2.52 mmol) was added in several portions over 4h. The mixture was stirred at room temperature for 3days, and then was poured into methanol. The resulting black polymeric material collected by suction filtration and Soxhlet-extracted with water for three days and methanol for three more days. It was then dried over P_2O_5 under reduced pressure at 120°C for 72 h to give the product in quantitative yield. Anal. Calcd. for $C_{15.39}H_9NO_2$: C, 77.07%; H, 3.75%; O, 13.34%. Found: C, 77.82%; H, 3.86%; O, 12.97%. FT-IR (KBr, cm^{-1}): 3441, 3384 (NH_2), 3027, 1647 (C=O), 1581, 1384, 1239, 1165.

HBP-PEK/VGCNF blends (10 wt% VGCNF; 7): Into a 100 mL three-necked, round-bottomed flask equipped with a magnetic stir-bar and nitrogen inlet, **HBP-PEK** (**3a,** 1.786 g), VGCNF (0.214 g) and methanesulfonic acid (MSA; 50 mL) were charged and heated at 50 °C for 24 h. The mixture was allowed to cool to room temperature and poured into water. The resulting black powder was collected by suction filtration, and Soxhlet-extracted with water for three days and methanol for three days. It was then dried over P_2O_5 under reduced pressure at 120°C for 72 h to give the product in quantitative yield. Anal. Calcd. for $C_{16.39}H_8O_4$: C, 73.22%; H, 2.98%; O, 23.81%. Found: C, 72.45%; H, 3.22%; O, 25.75%.

Results and Discussion

The as-received VGCNF contains a significant amount of hydrogen (about 1 wt%) based on the elemental analysis result and IR spectral data. This hydrogen content is presumably attributable to the sp^3C-H and sp^2C-H defects as methane is used as the major component in the feedstock for the VGCNF production. Previously, we demonstrated that vapor-grown carbon nanofibers could be functionalized via Friedal-Crafts acylation with a model compound, 2,4,6-trimethylphenoxybenzoic acid in polyphosphoric acid (PPA)/P_2O_5.[10a] The degree of functionalization, i.e. the number of defect C-H sites that were arylcarbonylated per 100 carbon, was determined to be ~ 3 atom% by the combination of TGA and elemental analysis results.

Thus, the *in-situ* polymerization of the A_2B monomer, 5-phenoxyisophthalic acid (**2**), in the presence of dispersed VGCNF was carried out with varied VGCNF content (0, 1, 2, 5, 10, 20, 30, 40 wt%) to yield the carboxylic-acid-terminated (HBP-PEK)-*g*-VGCNF (**3a-h**) as shown in Scheme 1. In a typical preparation, VGCNF and the A_2B monomer were first mechanically stirred and dispersed into PPA at 130 °C for 4 h. P_2O_5 was then added to enhance the acidity and catalytic potency of PPA to accelerate the polymerization and grafting of A_2B monomer to VGCNF surfaces, which most likely took place concurrently. The homogenous solutions became viscous overnight and polymerization mixture (dopes) stuck to the stirring rod at the end of each synthesis run. Previously, when a linear PEK analog was synthesized with VGCNF in attendance, the maximum amount of VGCNF incorporated into nanocomposites was 30 wt% because the viscosity was too high to render the mechanical stirring useless during the last stage of polymerization.[10b] However, in this work, up to 40 wt% (HBP-PEK)-*g*-VGCNF had been prepared without any stirring difficulty caused by the high viscosity. We attribute this improvement to the non-entangling nature of hyperbranched PEK. For comparison purposes, a 10 wt% physical blend (**7**) of HBP-PEK (**3a**) and VGCNF (**1**) was also prepared by mixing both in methanesulfonic acid (MSA) at 50 °C

[Scheme 1]

The presence of myriad carboxylic groups at the periphery of HBP-PEK provided an opportunity to evaluate the feasibility in post-polymer functionalization, and the change in the physical properties resulted from such chain-end modification. Thus, carboxylic-acid-terminated (HBP-PEK)-g-PEK (**3e**, 10 wt% of VGCNF) was further functionalized with a benzothiazole (**4**), a dodecyl ester (**5**) and an aromatic amine (**6**), respectively, under appropriate reaction conditions (Scheme 1). Thus, **3e** was condensed with *o*-aminothiophenol in PPA/P_2O_5 at 150 °C to afford the benzothiazole-terminated (HBP-PEK)-*g*-VGCNF (**4**). **3e** was esterified with 1-dodecanol in presence of N,N'-dicyclohexylcarbodiimide (DCC) as a dehydrating agent and 4-(N,N'-dimethylamino)pyridine (DMAP) as a catalyst to give the dodecylester-teminated (HBP-PEK)-*g*-VGCNF (**5**). The amine-terminated analog (**6**) was obtained via a Schmidt reaction by treating **3e** with sodium azide in MSA.[21]

Infrared Spectroscopy. The IR spectra of VGCNF, HBP-PEK and (HBP-PEK)-*g*-VGCNF are shown in Figure 1. The IR spectra of HBP-PEK and (HBP-PEK)-*g*-VGCNF are practically identical with respect to a peak-to-peak comparison. There are two types of carbonyl absorptions, i.e., the keto-carbonyl band at 1659 cm^{-1} and carboxylic-acid carbonyl band at lower frequency, 1720 cm^{-1}, in both HBP-PEK and (HBP-PEK)-*g*-VGCNF. The broad peak from 2500 to 3500 cm^{-1} is attributed to O-H stretch of carboxylic-acid group. Upon condensation with *o*-aminothiophenol in PPA/P_2O_5 medium, the carboxylic acid group was converted to benzothiazole as indicated by the disappearance of the broad OH band associated with COOH absorption at 2500-3500 cm^{-1}, and carboxylic acid carbonyl band at 1720 cm^{-1}, together with the concomitant appearance of the benzothiazole band at 1604 cm^{-1} (Figure 2b). Figure 2c shows the IR spectrum of dodecyl derivative, where the new bands at 2925 and 2854 cm^{-1} are assigned to C-H vibration of methylene groups. The carbonyl absorption is also shifted from 1720 cm^{-1} (carboxylic C=O) to 1703 cm^{-1} (carboxylic ester C=O). In MSA, it is believed that the reactive acylium intermediate derived from the carboxylic acid reacted with HN_3 to form the corresponding protonated acyl azide, which rearranged intramolecularly to form a protonated isocyanate. Upon acidic hydrolysis work-up, the isocyanate was converted to the resulting amine with the concomitant expulsion of CO_2.[22] Thus, the disappearance of C=O band at 1720 cm^{-1} and appearance of a weak NH_2 stretch at 3384 cm^{-1} are in accord with the occurrence of Schmidt reaction (Figure 2d). The amine absorption is weak due to its overlap with the magnified "moisture band" in KBr pellet around 3200-3400 cm^{-1}, stemming from the residual water molecules trapped in the crystal lattices, despite prolonged drying at 120^oC in an oven.

[Figure 1]

[Figure 2]

Solubility. The nanocomposites containing 1-40 wt% VGCNF were not soluble/dispersible in non-polar solvents, such as dichlorobenzene or toluene but were quite soluble/dispersible in aprotic solvents, such as NMP and DMAc. For example, the 10 wt% (HBP-PEK)-*g*-VGCNF could be dissolved in NMP up to 5 wt% to form visually clear, stable solution. It was only slightly soluble in ethanol, but totally soluble in ethanol/triethylamine (v/v 4:1) mixture, (Figure 3). However, all (HBP-PEK)-*g*-VGCNF samples were readily dissolved in

aqueous ammonia solution due to the ionization of the numerous surface CO_2H groups. The solution was clear and homogenous after months of standing under room conditions. On the other hand, the VGCNF of the blend sample **7** was easily separated by precipitation from all the solvents for HBP-PEK except MSA. As expected, the solubility/dispersibility of (HBP-PEK)-based nanocomposites was much improved in comparison with their linear mPEK-based counterparts, whose practical solubilility in strongly acidic solvent such as MSA was noted previously.[10b]

[Figure 3]

The organo-solubility of these (HBP-PEK)-based nanocomposites could be further manipulated by simple chain-end modification with appropriate end-capping agents. In this way, the benzothiazole-terminated nanocomposite (**4**) was soluble not only in polar solvents, but also in nonpolar solvents, such as dichlorobenzene and toluene since the benzothiazole groups are less polar than the carboxylic acid groups. Furthermore, when the chain-ends were transformed into the dodecylester groups, the solubility of the resulting nanocomposite (**5**) also changed dramatically; it could be even dissolved in chloroform instead of polar solvents such as DMF and DMSO, obviously promoted by the highly nonpolar, long alkyl chains. The amine-terminated nanocomposite (**6**) showed the similar solubility as the nanocomposite **3**. They were all soluble in polar solvents, such as NMP and DMAc. The solubility results were summarized in Table 1.

[Table 1]

Intrinsic Viscosity. The hyperbranched PEK, which contained a large number of terminal carboxylic acid groups, could not be analyzed directly by GPC, because the polymer adsorbed to the column, resulting in an incomplete elution. Shu *et al.* overcame this problem by esterification the carboxylic acid groups with methanol.[18] Since both the HBP-PEK and (HPB-PEK)-g-VGCNF nanocomposites were soluble in aprotic solvents, their intrinsic viscosities were determined in NMP. After their NMP solutions had been filtered through glass filters, the filtrates were used to measure the reduced and inherent viscosities. Lithium bromide was used to suppress the known polyelectrolyte effect stemming from the carboxylic acid groups. Thus, no polyelectrolyte effect was observed in our viscosity experiments. The intrinsic viscosities were determined from the extrapolation of reduced and inherent viscosities to the origin. The intrinsic

viscosity has been used to correlate the molecular weights of rigid-rod polymers, such as aromatic polyimides, poly(benzobisoxazoles) poly(benzobisimidazoles) and poly(benzobisthiazoles), which are insoluble in common GPC solvents (THF and NMP). The hyperbranched PEK displayed a viscosity [η] of 0.34 dL/g at 30 °C. As the amount of VGCNF increased, the [η] values of the nanocomposites were increased to 1.46 dL/g for 40 wt% (HBP-PEK)-*g*-VGCNF, which indicated that after the PEK had been attached to VGCNF, the molecular weights of the nanocomposites increased dramatically. The intrinsic viscosities of benzothiazole-terminated, dodecyl-terminated and amine-terminated (HBP-PEK)-g-VGCNF ranged from 0.56 to 0.67 dL/g (Table 2).

[Table 2]

Thermal Properties. The glass transition (T_g) temperatures were determined by DSC. The powder samples were first heated to 300 °C in a DSC chamber and cooled to 25 °C under a nitrogen purge to eliminate samples' thermal history. Then, the samples were heated to 300 °C again and T_g values were taken as the mid-point of the maximum baseline shift from second heating run. The hyperbranched homopolymer, HBP-PEK, exhibited a T_g of 227 °C. In addition, the same T_g value was also observed for a physical blend containing 10 wt% of as-received VGCNF. In the cases of *in-situ* nanocomposites, a single T_g was observed for all samples. In addition, when the VGCNF amount was increased, their T_g's were monotonously increased from 227 °C to 248 °C for 40 wt% (HBP-PEK)-*g*-VGCNF (Figure 4). In our previous work, when linear *m*PEK was grafted to VGCNF, similar results were also obtained.[10b] As the flexible polymer chain was attached to the rigid VGCNF surface, its mobility was constrained, and the T_g's had increased as much as 21 °C.

After the nanocomposite **3e** (T_g = 235 ^oC) had been endcapped with benzothiazole functionality, the T_g of the derivative nanocomposite **4** decreased to 184 °C. The T_g of the dodecyl-terminated nanocomposite **5** was further lowered to 81 °C since the non-polar dodecyl chains could also act as an internal plasticizer outside the polymer's periphery, which had reduced the glass transition temperature as much as 154 °C. The amine-terminated (HBP-PEK)-g-VGCNF contained about 10 wt% of VGCNF. Its T_g of 242 °C was similar to the carboxylic terminated analog (Figure 5 and Table 3).

[Figure 5]

[Table 3]

As we have shown previously, the combination of a model reaction, TGA experiments and elemental analysis is a simple, yet powerful method to quantify the degree of functionalization as well as the VGCNF and PEK compositions in the nanocomposites. VGCNF exhibited an expectedly high thermal stability. Its 5 wt% weight loss ($T_{d5\%}$) occurred at 723 °C in air and higher than 900 °C in nitrogen. HBP-PEK and (HBP-PEK)-*g*-VGCNF nanocomposites displayed $T_{d5\%}$ in the range of 486-426 °C in air and 379-420 °C in nitrogen, respectively (Figure 6). The char yield at 650 °C in air, after HBP-PEK had been thermooxidatively stripped off, was used to determine the amount of VGCNF originally present in the nanocomposites. Excellent agreement was obtained between the theoretical and experimental values for all the HBP-PEK/VGCNF compositions (Table 2).

[Figure 6]

TGA results of chain-end modified (HBP-PEK)-g-VGCNF nanocomposites (**4**, **5** and **6**) are shown in Figure 7 and Table 3. Benzothiazole-terminated (HBP-PEK)-*g*-VGCNF exhibited the highest $T_{d5\%}$ (429 °C in air and 432 °C in nitrogen) since the benzothiazole group is most thermally and thermo-oxidatively stable among the end-group functionalities used in this work. The thermal stability of **5** was the lowest due to its alkyl end-groups. The amine-terminated (HBP-PEK)-*g*-VGCNF **6** show similar thermal stability to **3**. After chain-end modification of the 10 wt% HBP-PEK)-*g*-VGCNF had been accomplished with benzothiazole, alkyl and amine groups, the theoretical VGCNF contents were changed accordingly to 7.9, 6.9 and 11.8 wt%, respectively. The char yields of **4**, **5** and **6** at 650 °C are 8.2, 6.9 and 10.3 wt%, which agree well with the respective theoretical values (Table 2).

[Figure 7]

Nuclear Magnetic Resonance (NMR): The greatly improved solubility of (HBP-PEK)-g-VGCNF nanocomposites in organic solvents provided a rare opportunity for solution NMR studies of polymer-modified carbon-based nanomaterials. While there are reports for the solution NMR studies/spectra of SWNT and MWNT,[23] to our knowledge, none have been

reported for chemically-modified VGCNF. Thus, the NMR characterization was carried out in deuterated DMSO. The solution phase ^{1}H NMR spectrum of 10wt% (HBP-PEK)-g-VGCNF is compared with that of pristine HBP-PEK in Figure 8. Except for being broader, the aromatic proton peaks in (HBP-PEK)-g-VGCNF are generally similar to those in free HBP-PEK. For the VGCNF-attached PEK, the proton signals are much broader, as commonly observed in the NMR characterization of solubilized carbon nanotubes. The considerable signal broadening for the HPK-PEK upon functionalizing with VGCNF could in principle be explained in terms of two different mechanisms: the attachment of the HBP-PEK to nanofibers vs the effect of possible paramagnetic impurities in the solution. The latter is obviously relevant to the VGCNF containing samples because of the possibility of residual metal catalysts. The as-received VGCNF used in this experiment had been heat-treated, and its iron content is less than 100 ppm. There was some evidence that PPA was quite effective in removing metal impurity during the reaction.[24] We have measured the proton spin-lattice (T_1) and spin-spin (T_2) relaxation times to determine if residual paramagnetic impurities make a significant contribution to the line widths for the grafted CNF's. Paramagnetic impurities greatly increase both the T_1's and T_2's and can therefore affect the line widths. The polymers grafted to CNF's are slowly tumbling macromolecules and are expected to have long (seconds) relaxation times, so any paramagnetic contribution should be easily detected. The proton T_1's measured by inversion-recovery for the 10 wt% (HBP-PEK)-g-VGCNF in DMSO-d_6 were 3.93 and 6.81 s for the peaks at 7.8 and 7.1 ppm, respectively. These long T_1's rule out any significant contribution from paramagnetic impurities. Another experiment was conducted to clarify this issue. The 10 wt% HBP-PEK/VGCNF blend was dispersed in deuterated DMSO by sonication. The mixture showed good dispersion in DMSO (Figure 10). However, its proton signals do not show any broadness compared with those of free HBP-PEK. Therefore, the observed broad proton signals are most probably stemming from the high molecular weight and low mobility of HBP-PEK after it has been grafted onto VGCNF. (HBP-PEK)-g-VGCNFs were readily soluble in deuterated DMSO without any sonication and its solution was stable on the bench for months. In the case of the blend, the VGCNF was precipitated out from DMSO a week after sonication (Figure 9), which further proves that VGCNF was solubilized with aid of the covalently bonded HPB-PEK. Overall, the results provide another piece of evidence to strongly support that VGCNT has been grafted with relatively high molecular weight HPB-PEK.

[Figure 8]

[Figure 9]

Scanning Electron Microscopy (SEM). The SEM image of pristine VGCNF shows that most of the tube surfaces are clean as shown in Figure 10(a). Some of the nanotube surfaces display "stacked Dixie cups" or bamboo texture. The average diameter is in the range of 100-200nm. In order to investigate the effect of PPA/P_2O_5 on VGCNF, a control experiment was run where VGCNF without TMPBA was heated in PPA/P_2O_5 at 130 °C for three days to afford a PPA-treated sample (PT-VGCNF) in 94% recovery yield. The work-up was the same as that for (HPB-PEK)-g-VGCNF. PT-VGCNF has slightly lower carbon and hydrogen contents than pristine VGCNF, although the differences are in the range of experimental errors. The pristine and PPA-treated VGCNF share the same morphologies including surface, diameter and length, Figure 10(b). This confirms that PPA/P_2O_5 is indeed a mild, non-destructive medium for F-C reactions on carbon nanosurfaces. The surfaces of 10 wt% and 20 wt% (HBP-PEK)-*g*-VGCNF are highly coated with the polymer and the original VGCNF texture such as stacked Dixie cups was lost due to the polymer grafting as shown in Figure 10(c) and (d). The average diameters of (HBP-PEK)-*g*-VGCNF increased slightly. The morphology of 10 wt% VGCNF/HBP-PEK physical blend, **7,** was also investigated using SEM. The elemental analysis results of **7** and **3e** are similar (Table 2), indicative of both containing similar components. However, large clusters of aggregate VGCNF were observed under SEM as shown in Figure 10(e). Furthermore, the VGCNF surface, as shown in Figure 10(f), was obviously clean without any tethered polymer, which confirmed that **7** was indeed a physical blend.

[Figure 10]

Transmission Electron Microscopy (TEM): The TEM image of pristine VGCNF shows that the nanofiber surface is smooth (Figure 11). However, the nanofiber surfaces of 20 wt% (HBP-PEK)-*g*-VGCNF are rough and fuzzy, and there is an obvious increase in the diameter as well. We attribute this diameter increase to the heavy coating by the hyperbranched PEK (thickness of approximately 10-20nm).

[Figure 11]

Conclusions

Our results show that (HBP-PEK)-g-VGCNFs have considerably better solubility (e.g. in aprotic polar solvents) than their linear analogs, *m*PEK-g-VGCNF, validating our concept in using an aromatic hyperbranched structure to enhance organo-solubility/dispersibility and widen the processing options of CNF/CNT materials. Because of the generally much lower viscosity behaviors as an attribute of hyperbranched polymers, the derived nanocomposites would be amenable to applications where speed and large-area coverage are required, e.g. spraying and painting techniques. In addition, we also show that the overall polarity of the nanocomposites could be synthetically controlled by converting the terminal CO_2H groups of the HBP-PEK grafts to amine, benzothiazole groups, and dodecyl esters groups. The former two cases could be conducted in a one-pot fashion by the addition of the respective endcapping agents after the A_2B polymerization in PPA has completed. A complementary approach that we have demonstrated to be successful in such polarity modification is via an *in-situ* A_3+B_2 polymerization with judicious stoichiometric variation of the triacid (A_3) and bis(phenyether), B_2 monomers.[25] As expected, the nature of chain ends can dramatically affect physical properties of the resulting nanocomposites. For example, the dodecyl-terminated nanocomposite displayed an excellent solubility in chloroform and a much lower T_g than the CO_2H-terminated analog. Perhaps, most importantly, we have demonstrated that aromatic hyperbranched polymers with its vast number of end-groups and random structures can be a very useful tool in enhancing solubility/nano-dispersibility, introducing application-specific functionality (e.g. lithium-hydrogen exchange for ion conductivity and battery applications), and modulating thermal properties of the polymer nanocomposites with high contents of CNF/CNT materials for higher temperature applications.

Acknowledgement

We are grateful to Sharon Simko (University of Dayton Research Institute) for their assistance in monomer synthesis; Marlene Houtz and Gary Price (both of University of Dayton Research Institute) for acquiring TGA and SEM data and images. This project was supported by funding from Wright Brother Institute (Dayton), Office of Scientific Research (AFOSR) and Materials & Manufacturing Directorate, US Air Force Research Laboratory.

List of Scheme

List of Tables

List of Figures

one week on the bench; (d) 10 wt% (HBP-PEK)-g-VGCNF after one week standing on a lab bench.

Figure 10. SEM images of (a) pristine VGCNF (x50k); (b) PPA/P_2O_5 treated VGCNF (x25k); (c) 10 wt% (HBP-PEK)-g-VGCNF (x50k); (d) 20 wt% (HBP-PEK)-g-VGCNF (x50k); (e) 10 wt% (HBP-PEK)/VGCNF blend (x10k); 10 wt% (HBP-PEK)/VGCNF blend (x40k).

Figure 11. TEM images of (HBP-PEK)-g-VGCNF (a) pristine VGCNF; (b) 20 wt% (HBP-PEK)-g-VGCNF.

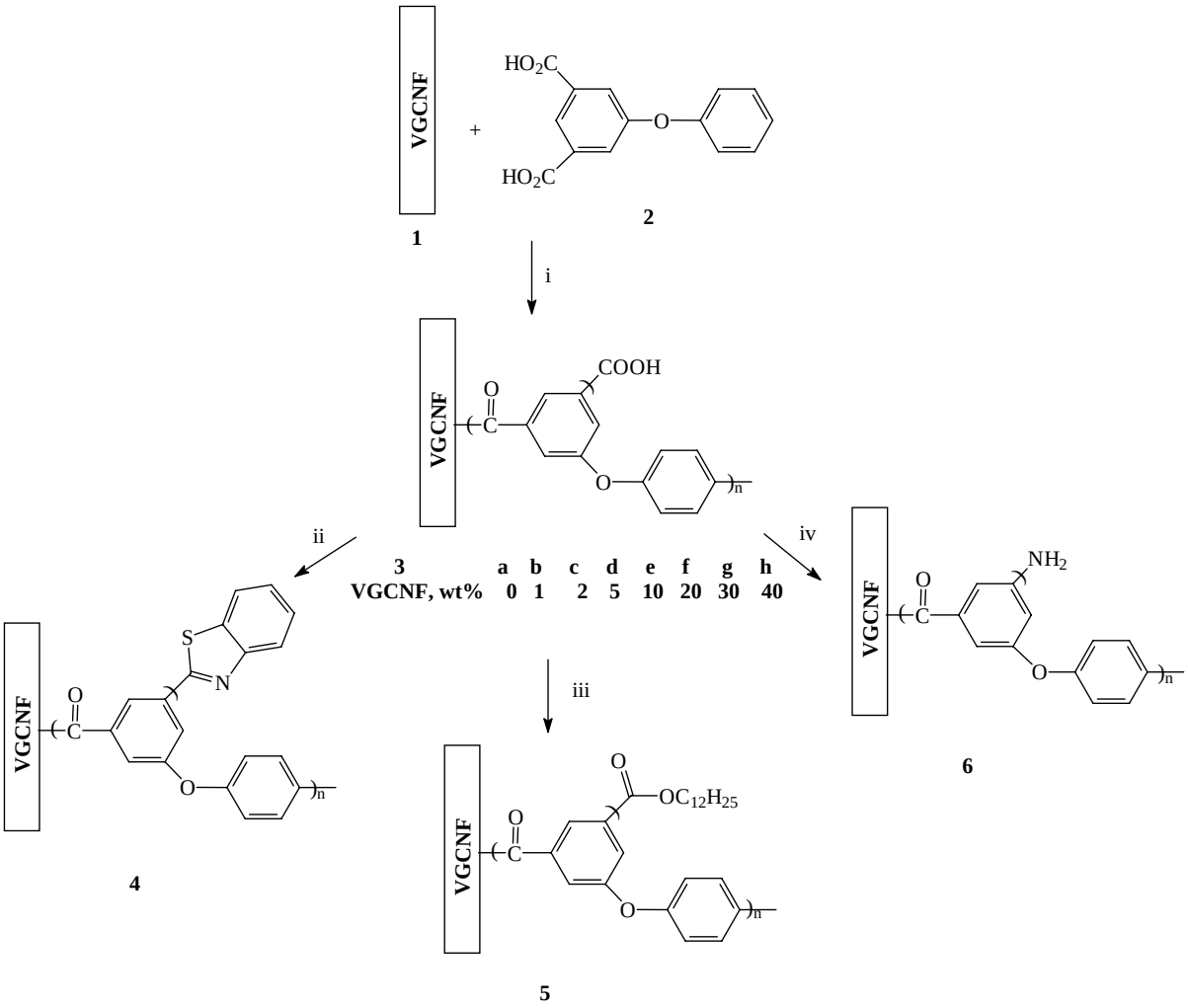

Scheme 1. *In-situ* polymerization of 3,5-diphenoxybenzoic acid with VGCNF and its post-polymer functionalization: i. PPA/P_2O_5, 130 °C; ii. PPA/P_2O_5, 2-aminothiophenol, 150 °C; iii. 1-dodecanol, DCC, DMAP, DMF; iv. sodium azide, MSA.

Table 1. Solubility testing results of (HBP-PEK)-g-VGCNF

Sample	MSA	NMP	DMAc	Ethanol	Ethanol/TEA	NH_4OH	DCB	$CHCl_3$
3a	+	+	+	±	+	+	–	–
3b	+	+	+	±	+	+	–	–
3c	+	+	+	±	+	+	–	–
3d	+	+	+	±	+	+	–	–
3e	+	+	+	±	+	+	–	–
3f	+	+	+	±	+	+	–	–
3g	+	+	+	±	+	+	–	–
3h	+	+	+	±	+	+	–	–
4	+	+	+	±	–	–	+	–
5	–	–	–	–	–	–	+	+
6	+	+	+	±	–	–	–	–
7	+	–	–	–	–	–	–	–

+, soluble; ±, partially soluble; –, insoluble.
MSA: methanesulfonic acid; NMP: 1-methyl-2-pyrrolidinone; DMAc: dimethylacetamide; TEA: triethylamine; DCB: dichlorobenzene.

Table 2. VGCNF:A_2B monomer feed ratio, calculated and TGA-determined VGCNF:HBP-PEK composition, intrinsic viscosity and elemental analysis data

	Feed		Calculated		Found[a]		Elemental Analysis			
Sample	VGCNF (wt%)	HBP-PEK (wt%)	VGCNF (wt%)	HBP-PEK (wt%)	VGCNF (wt%)	$[\eta]^b$(dL/g)		C (%)	H (%)	O (%)
1	100	0	100	0	99.8	-	Calcd[c]	100	0	0
							Found	99.02	1.01	<0.1
3a	0	100	0	100	0.7	0.34	Calcd[c]	70.00	3.36	26.63
							Found	69.54	3.47	26.23
3b	1	99	1.1	98.9	1.4	0.42	Calcd[c]	70.34	3.32	26.34
							Found	69.60	3.29	27.01
3c	2	98	2.2	97.8	2.6	0.47	Calcd[c]	70.67	3.29	26.04
							Found	70.47	3.32	26.23
3d	5	95	5.4	94.6	5.2	0.57	Calcd[c]	71.62	3.15	25.22
							Found	71.48	3.10	23.93
3e	10	90	10.7	89.3	11.0	0.82	Calcd[c]	73.22	2.98	23.81
							Found	72.94	3.12	21.74
3f	20	80	21.2	78.8	22.1	0.91	Calcd[c]	76.37	2.63	21.00
							Found	76.08	2.79	19.55
3g	30	70	31.5	68.5	31.3	0.87	Calcd[c]	77.88	2.32	18.39
							Found	77.53	2.23	18.81
3h	40	60	41.8	58.2	42.1	1.46	Calcd[c]	82.00	2.01	15.99
							Found	81.82	2.10	16.47
4	7.1	92.9	7.9	92.1	8.2	0.64	Calcd[c]	71.92	2.94	12.84
							Found	72.44	3.18	12.53
5	6.4	93.6	6.9	93.1	6.9	0.56	Calcd[c]	78.03	7.32	14.65
							Found	78.54	7.61	13.93
6	11.1	88.9	11.8	88.2	10.3	0.67	Calcd[c]	77.07	3.75	13.34
							Found	76.81	3.88	12.97
7	-	-	10.7	89.3	10.2	-	Calcd[c]	73.22	2.98	23.81
							Found	72.45	3.22	25.75

[a] Residual weight percentage at 650 °C from TGA thermograms in air. [b] Intrinsic viscosity measured in NMP at 30.0±0.1°C. [c] A_2B repeat unit $C_{14}H_8O_4$ and calculated repeat unit as followed: **3a** (100:0) $C_{14}H_8O_4$; **3b** (1:99) $C_{14.23}H_8O_4$; **3c** (2:98) $C_{14.45}H_8O_4$; **3d** (5:95) $C_{15.13}H_8O_4$; **3e** (10:90) $C_{16.39}H_8O_4$; **3f** (20:80) $C_{19.38}H_8O_4$; **4g** (30:70) $C_{22.59}H_8O_4$; **3f** (40:60) $C_{27.33}H_8O_4$; **5** $C_{22.39}H_{11}NO_3S$; **6** $C_{28.39}H_{32}O_4$; **7** $C_{15.39}H_9NO_2$.

The formula of (HBP-PEK)-g-VGCNF is $C_{14+n}H_8O_4$. $C_{14}H_8O_4$ is the formula of PEK repeat unit. Sub n is numbers of VGCNF carbons per PEK repeat unit and calculated as followed:

$$n = \left(\frac{\text{Weight percentage of VGCNF}}{12.011}\right) \Big/ \left(\frac{\text{Weight percentage of HBP-PEK}}{240.22}\right)$$

Where 12.011 is VGCNF formula (C) molecular weight and 240.22 is the molecular weight of HBP-PEK repeat unit

Table 3. Thermal properties of (HBP-PEK)-g-VGCNF

	Calculated Composition[a]		DSC	TGA			
				in nitrogen		in air	
Sample	VGCNF (wt%)	HBP-PEK (wt%)	T_g[b] (°C)	$T_{5\%}$[c](°C)	Char at 650 °C (wt%)	$T_{5\%}$[c](°C)	Char at 650 °C (wt%)
1	100	0	-	>900	99.7	723	99.8
3a	0	100	227	387	55.5	408	0.7
3b	1.1	98.9	231	383	56.2	417	1.4
3c	2.2	97.8	231	417	57.7	400	2.6
3d	5.4	94.8	232	379	65.3	386	5.2
3e	10.7	89.3	235	420	61.2	410	11.0
3f	21.2	77.9	241	419	66.8	426	22.1
3g	31.5	68.5	244	414	71.2	413	31.2
3h	41.8	58.2	248	405	75.5	412	42.1
4	7.9	92.1	184	432	63.0	429	8.2
5	6.9	93.1	81	377	54.8	356	6.9
6	11.8	88.2	242	398	65.8	394	10.6
7	10.7	89.3	227	414	60.4	402	10.2

[a] Calculation based on the assumption that VGCNF is 100% C and the molar mass of the repeat unit of HBP-PEK is 240.22. [b] Inflection in baseline on DSC thermogram obtained in N_2 with a heating rate of 10 °C/min. [c] Temperature at which 5% weight loss occurred on TGA thermogram obtained with a heating rate of 10 °C/min.

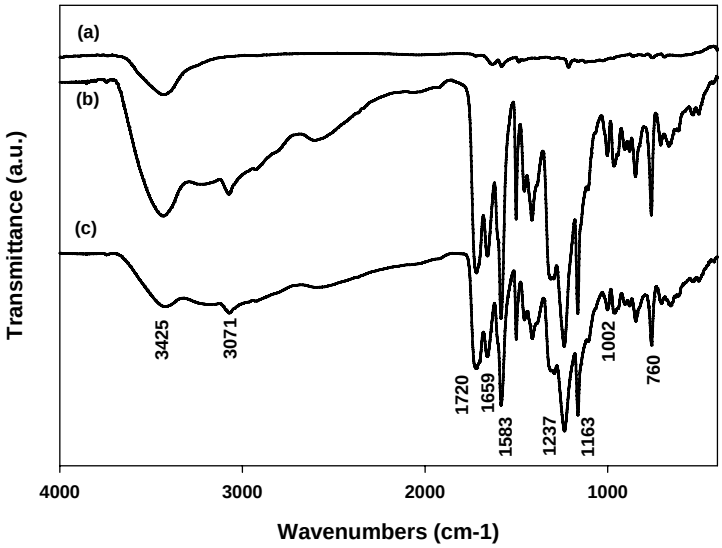

Figure 1. Composite FT-IR spectra of (a) VGCNF 5; (b) HBP-PEK 6a; (c) 10wt% (HBP-PEK)-g-VGCNF 6e.

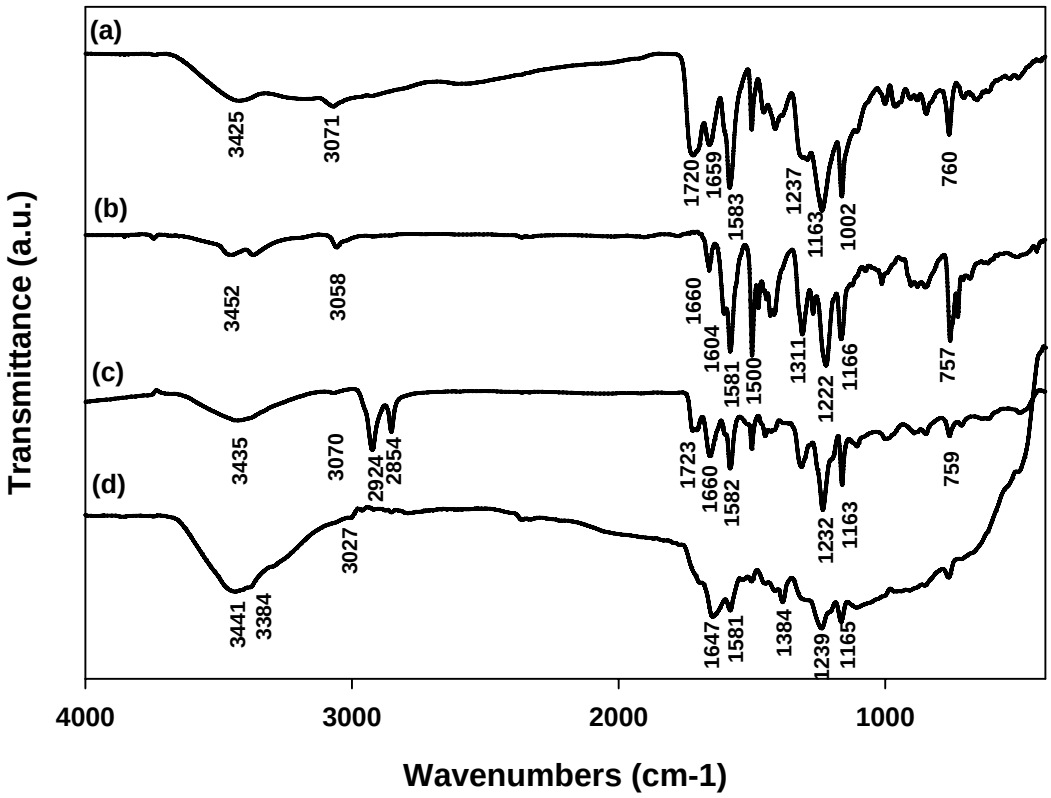

Figure 2. Composite FT-IR spectra of (HPB-PEK)-g-VGCNF. (a) carboxylic-acid-terminated, (b) benzothiazole-terminated, (c) dodecyl-terminated, (d) amine-terminated.

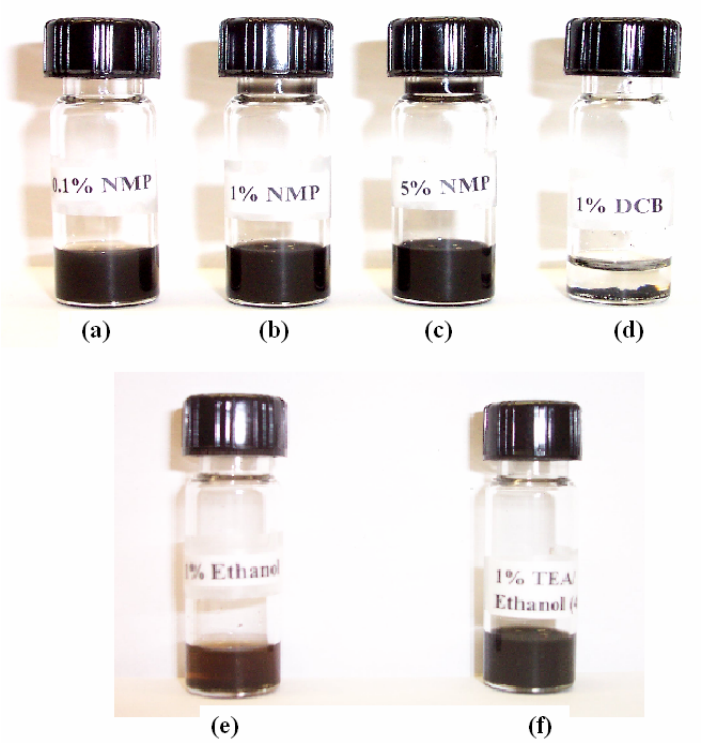

Figure 3. Solubility testing of compound 6c (a) 0.10 wt% in NMP; (b) 1.0 wt% in NMP; (c) 5.0 wt% in NMP; (d) 1.0 wt% in DCB; (e) 1.0 wt% in ethanol; (f) 1.0 wt% in ethanol/triethylamine.

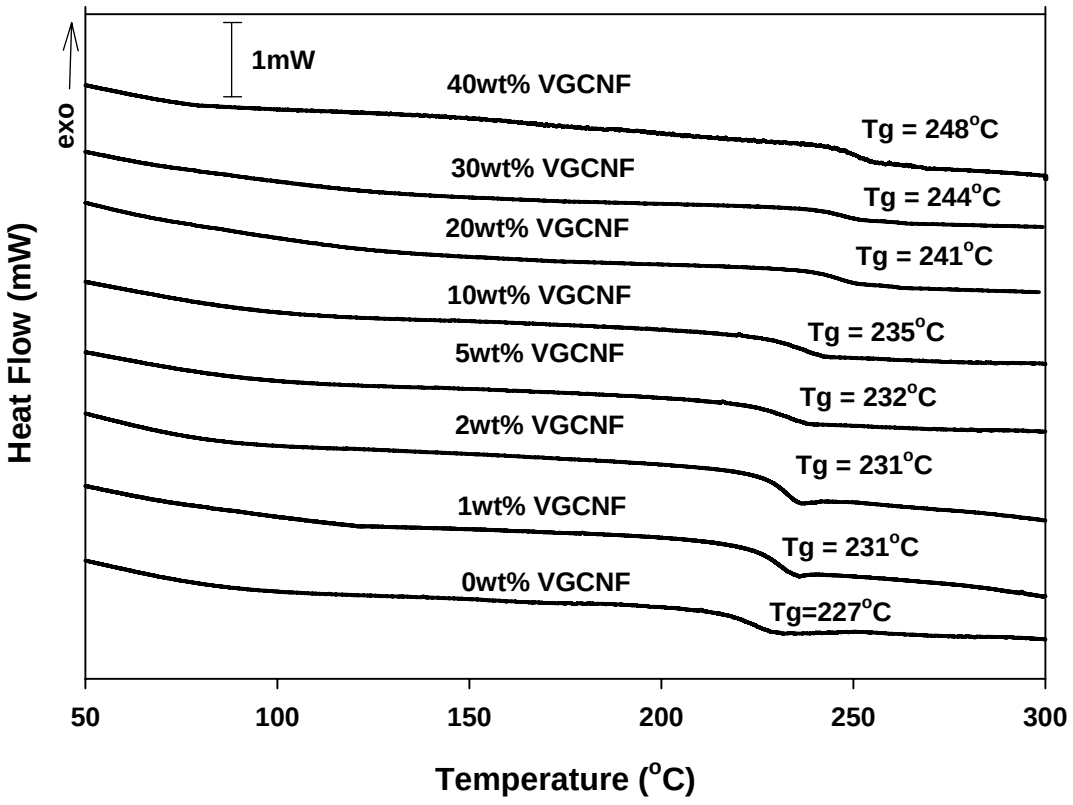

Figure 4. DSC thermograms of (HBP-PEK)-g-VGCNF samples scanned with a heating rate of 10 °C/min.

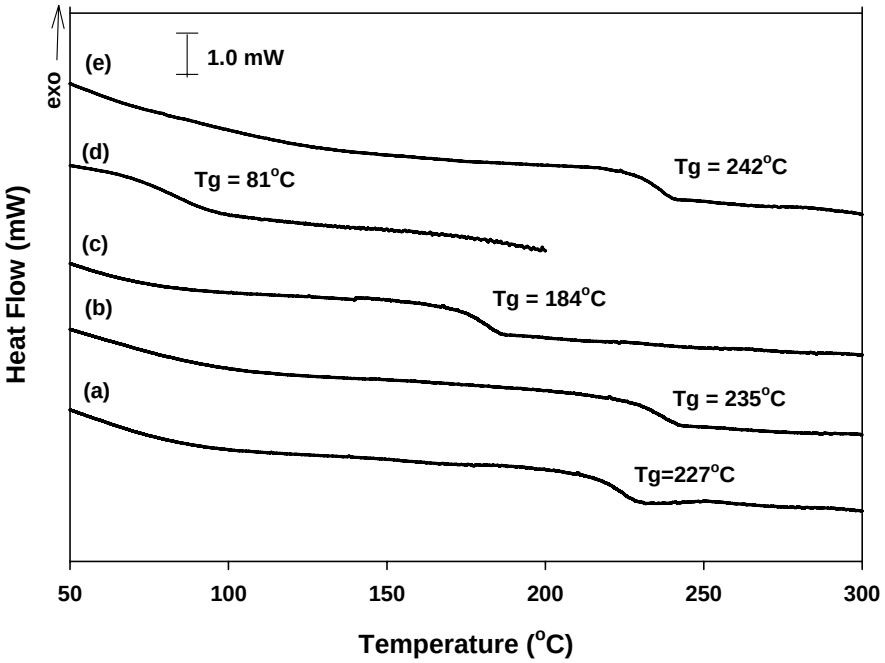

Figure 5. DSC thermograms of different end-capping (HPB-PEK)-g-VGCNF samples scanned with a heating rate of 10 °C/min (a) carboxylic-acid-terminated HPB-PEK, 0 wt% of VGCNF; (b) carboxylic-acid-terminated, 10.3 wt% of VGCNF, 6e; (c) benzothiazole-terminated, 8.2 wt% of VGCNF, 4; (d) Dodecyl-terminated, 6.9 wt% of VGCNF, 5; (e) amine-terminated, 10.6 wt% of VGCNF, 6.

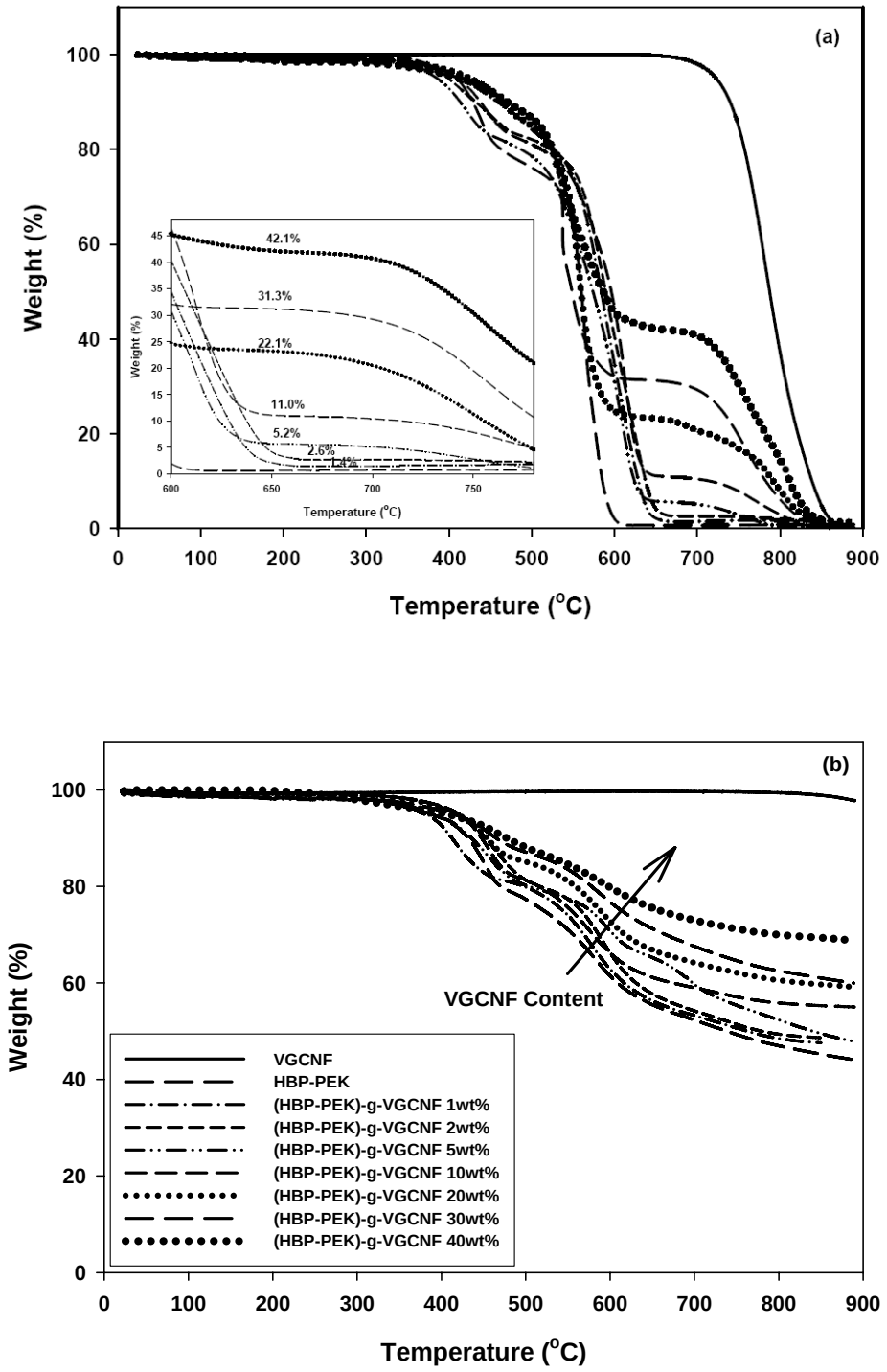

Figure 6. TGA thermograms of (HBP-PEK)-g-VGCNF samples scanned with a heating rate of 10 °C/min (a) in air; and (b) in nitrogen.

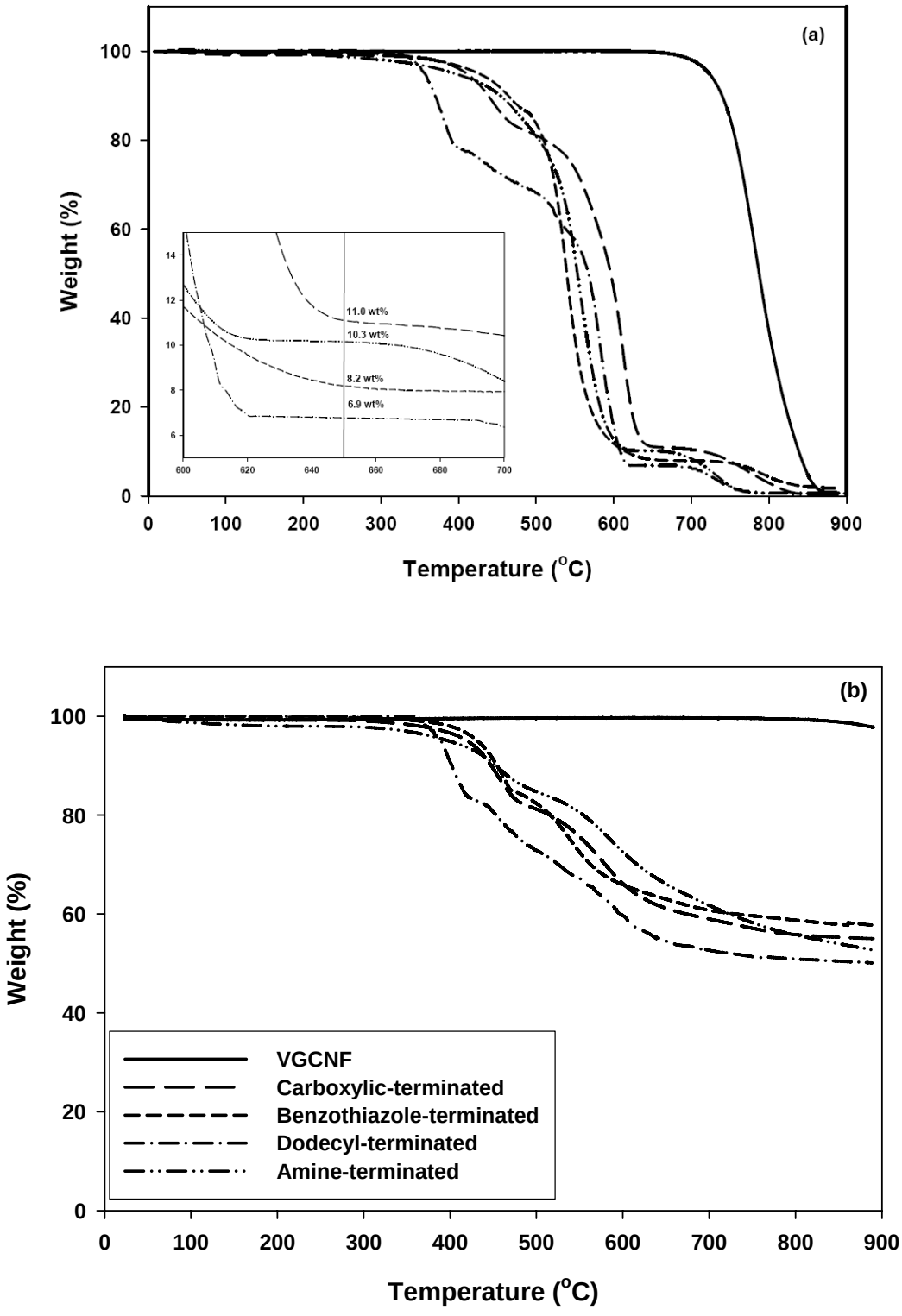

Figure 7. TGA thermograms of end-capped (HBP-PEK)-g-VGCNF samples scanned with a heating rate of 10 °C/min (a) in air; and (b) in nitrogen.

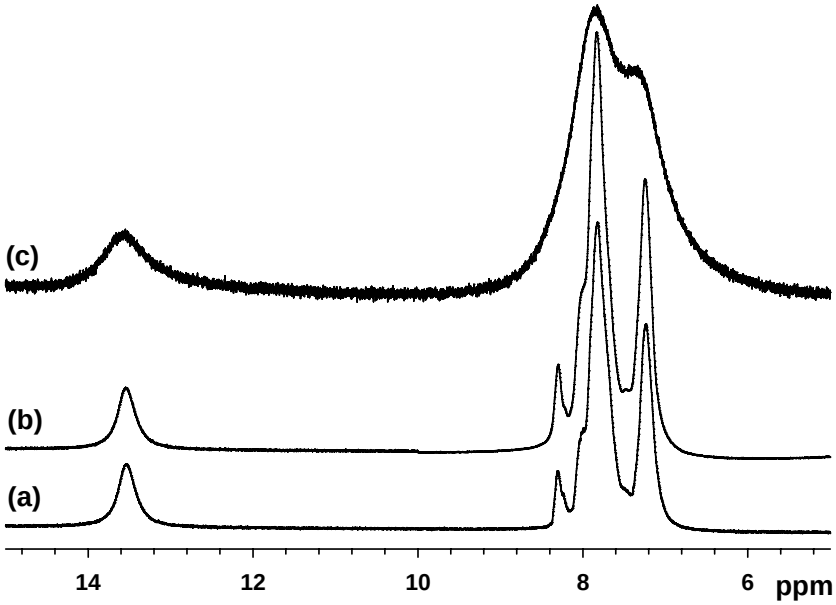

Figure 8. ^{1}H NMR spectra (DMSO-d_6) of (a) HBP-PEK; (b) 10wt% (HBP-PEK)/VGCNF blend; (c) 10wt% (HBP-PEK)-g-VGCNF.

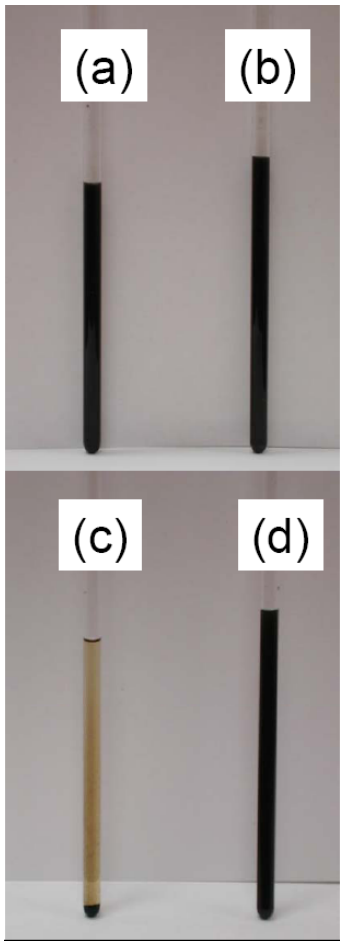

Figure 9. DMSO-d_6 solution of (a) 10 wt% VGCNF/(HBP-PEK)blend right after sonication; (b) 10 wt% (HBP-PEK)-g-VGCNF without sonication; (c) 10 wt% VGCNF/(HBP-PEK)blend after one week on the bench; (d) 10 wt% (HBP-PEK)-g-VGCNF after one week on the bench.

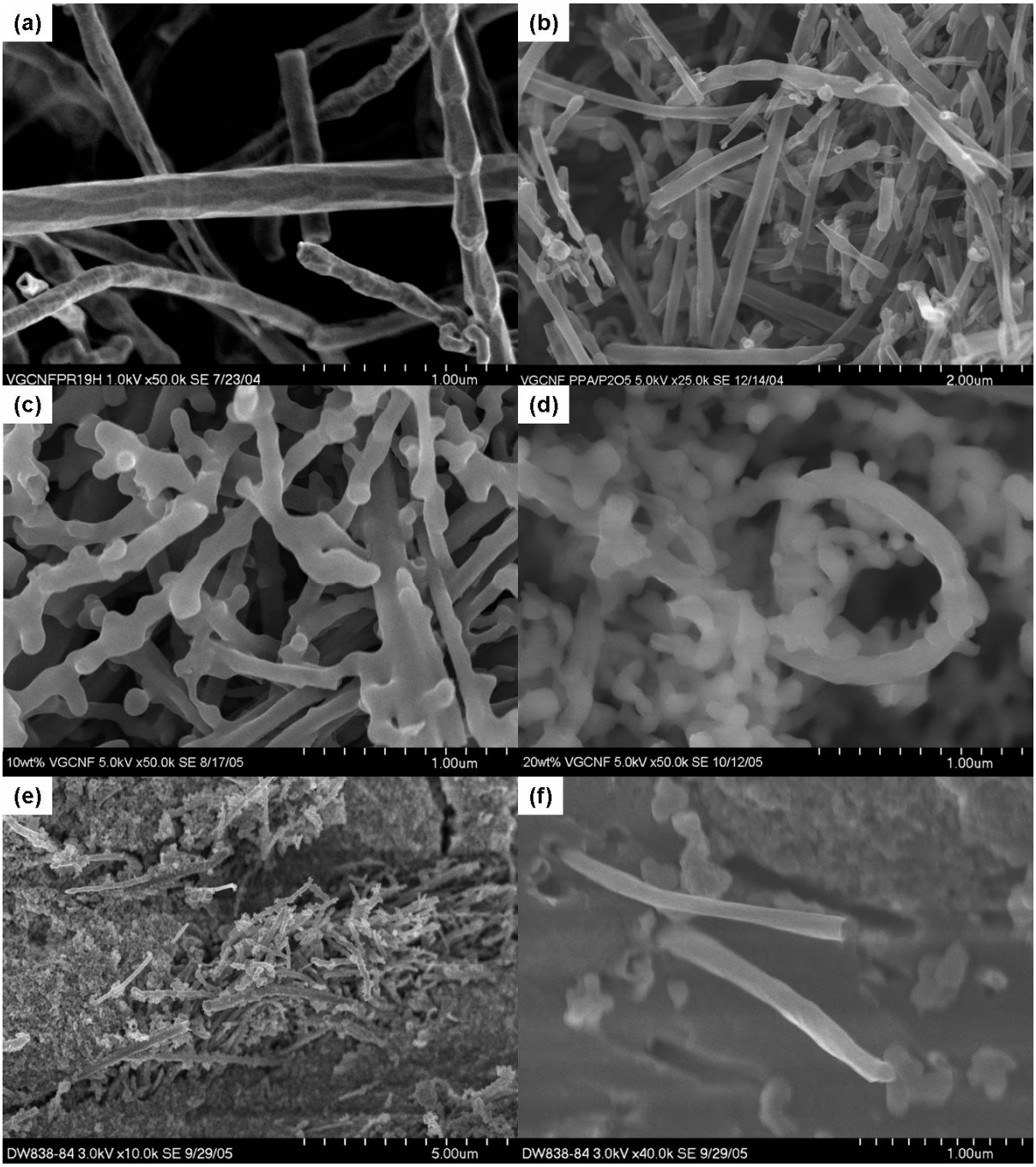

Figure 10. SEM images of (a) pristine VGCNF (x50k); (b) PPA/P_2O_5 treated VGCNF (x25k); (c) 10 wt% (HBP-PEK)-g-VGCNF (x50k); (d) 20 wt% (HBP-PEK)-g-VGCNF (x50k); (e) 10 wt% (HBP-PEK)/VGCNF blend (x10k); 10 wt% (HBP-PEK)/VGCNF blend (x40k).

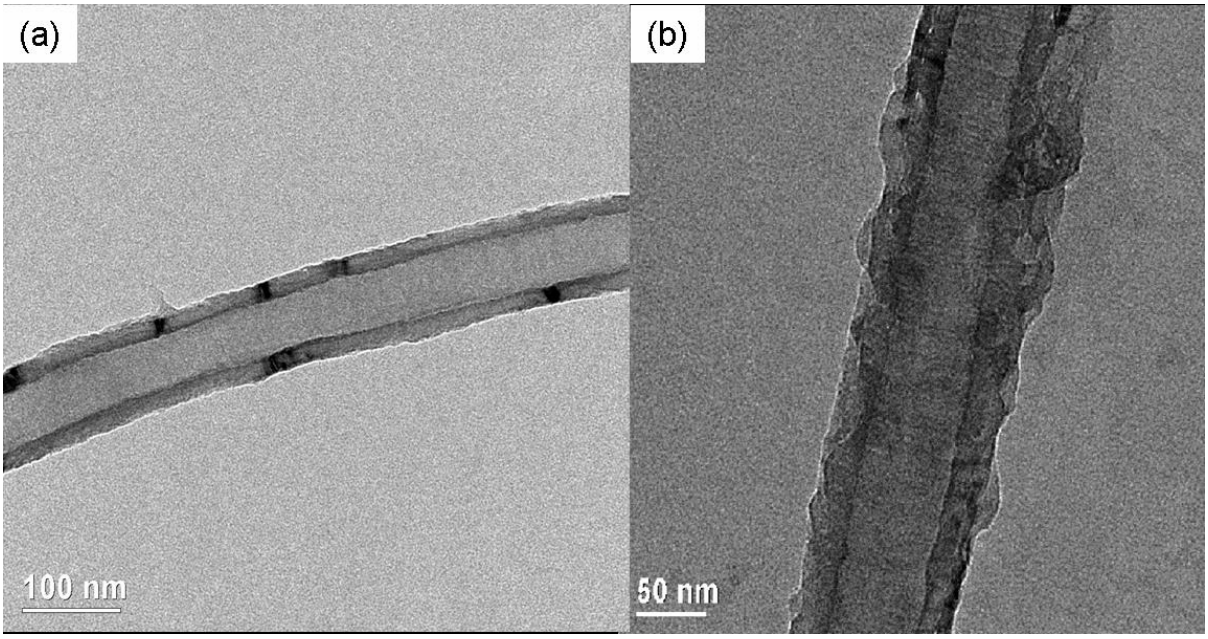

Figure 11. TEM images of (HBP-PEK)-g-VGCNF (a) pristine VGCNF; (b) 20 wt% (HBP-PEK)-g-VGCNF.

References

[1] Some recent reviews on SWNT and MWNT: (i) Mahar, B.; Laslau, C.; Yip, R.; Sun, Y. *IEEE Sens. J.* **2007,** 7, 266; (ii) Robertson, J. *Mater. Today (Oxford, U. K.)* **2007,** 10 (1-2), 36; (iii) Campidelli, S.; Klumpp, C.; Bianco, A.; Guldi, D. M.; Prato, M. *J. Phys. Org. Chem.* **2006,** 19, 531; (iv) See, C. H.; Harris, A. T. *Ind. Eng. Chem. Res.* **2007,** 46, 997; (v) Nakashima, N. *Sci. Technol. Adv. Mater.* **2006,** 7, 609; (vi) Avouris, P.; Chen, J. *Mater. Today (Oxford, U. K.)* **2006,** 9(10), 46; (vii) in het Panhuis, M. *J. Mater. Chem.* **2006,** 16, 3598; (viii) Snow, E. S.; Perkins, F. K.; Robinson, J. A. *Chem. Soc. Rev.* **2006,** 35, 790; (xi) Moniruzzaman, M.; Winey, K. I. *Macromolecules* **2006,** 39, 5194; (x) Lau, K.-T.; Gu, C.; Hui, D. *Composites, Part B* **2006,** 37B, 425.

[2] DWNT: (i) Bandow, S.; Takizawa, M.; Hirahara, K.; Yudasaka, M.; Iijima, S. *Chem. Phys. Lett.* **2001,** 337, 48; (ii) Hutchison, J. L.; Kiselev, N. A.; Krinichnaya, E. P.; Krestinin, A. V.; Loutfy, R. O.; Morawsky, A. P.; Muradyan, V. E.; Obraztsova, E. D.; Sloan, J.; Terekhov, S. V.; Zakharov, D. N. *Carbon* **2001,** 39, 761; (iii) Bacsa, R.R.; Peigney, A.; Laurent, Ch.; Puech, P.; Bacsa, W.S. *Phys. Rev., B* **2002**, 65, 161404; (iv) Nagy, C. L.; Diudea, M. V.; Balaban, T. S. *Nanostructures* **2005**, 25; (v) Sugai, T. *New Diamond Front. Carbon Technol.* **2006,** 16, 151; (v) Yamada, T.; Namai, T.; Hata, K.; Futaba, D. N.; Mizuno, K.; Fan, J.; Yudasaka, M.; Yumura, M.; Iijima, S. *Nat. Nanotechnol. 2***006,** 1, 131.

[3] FWNT: (i) Gohier, A.; Minea, T. M.; Djouadi, M. A.; Granier, A. *J. Appl. Phys.* **2007,** 101, 054317/1; (ii) Gohier, A.; Minea, T. M.; Djouadi, M. A.; Jimenez, J.; Granier, A. *Phys. E* **2007,** 37, 34; (iii) Qian, C.; Qi, H.; Liu, J. *J. Phys. Chem. C* **2007,** 111, 131; (iv) Qi, H.; Qian, C.; Liu, J. *Chem. Mater.* **2006,** 18, 5691; (v) Qian, C.; Qi, H.; Gao, B.; Cheng, Y.; Qiu, Q.; Qin, L.-C.; Zhou, O.; Liu, J. *J. Nanosci. Nanotechnol.* **2006,** 6, 1346; (vi) Ramesh, Palanisamy; Sato, Kenichi; Ozeki, Yuji; Yoshikawa, Masahito; Kishi, Naoki; Sugai, Toshiki; Shinohara, Hisanori. *NANO* **2006**, 207; (vii) Qian, C.; Qi, H.; Gao, B.; Zhou, O.; Liu, J. *PMSE Prepr.* **2005,** 92, 516.

[4] Applied Sciences, Inc. Cederville, OH, USA: http://www.apsci.com

[5]Rodriguez, N. M. *J. Mater. Res.* **1993,** 8, 233.

[6] Maruyama, B.; Alam, K. *SAMPE Journal* **2002,** 38, 59-70.

[7] Carneiro, O. S.; Covas, J. A.; Bernardo, C. A.; Caldeira, G.; Hattum, F. W. J. V.; Ting, J. M.; Alig, R. L.; Lake, M. L. *Comp. Sci. Technol.* **1998**, *58*, 401.

[8] Singh, C.; Quested, T.; Boothroyd, C. B.; Thomas, P.; Kinloch, I. A.; Abou-Kandil, A. I.; Windle, A. H. *J. Phy. Chem. B* **2002**, *106*, 10915.

[9] (a) Baek, J.-B.; Tan, L.-S. *Polymer* **2003**, *44*, 4135; (b) Baek, J.-B.; Park, S.-Y.; Price, G. E.; Lyons, C. B.; Tan, L.-S. *Polymer* **2005,** 46, (5), 1543.

[10] (a) Baek, J.-B.; Lyons, C. B.; Tan, L.-S. *J. Mater. Chem.* **2004**, *14*, 2052. (b) Baek, J.-B.; Lyons, C. B.; Tan, L.-S. *Macromolecules* **2004**, *37*, 8278; (c) Lee, H.-J.; Oh, S.-J.; Choi, J.-Y.; Kim, J. W.; Han, J.; Tan, L.-S.; Baek, J.-B. *Chem. Mater.* **2005,** 17, 5057; (d) Oh, S.-J.; Lee, H.-J.; Keum, D.-K.; Lee, S.-W.; Wang D.H.; Park, S.-Y.; Tan, L.-S.; Baek, J.-B. *Polymer* **2006**, *47*, 1132.

[11] Rhodes, S. M.; Higgins, B.; Xu, Y.; Brittain, W. J. *Polymer* **2007,** 48, 1500.

[12] (i) Gao, C.; Muthukrishnan, S.; Li, W.; Yuan, J.; Xu, Y.; Mueller, A. H. E. *Macromolecules* **2007,** 40, 1803; (ii) Cao, L.; Yang, W.; Yang, J.; Wang, C.; Fu, S. *Chem. Lett.* **2004,** 33, 490.

[13] Xu, Y.; Gao, C.; Kong, H.; Yan, D.; Jin, Y. Z.; Watts, P. C. P. *Macromolecules* **2004,** 37, 8846.

[14] Hong, C.-Y.; You, Y.-Z.; Wu, D.; Liu, Y.; Pan, C.-Y. *Macromolecules* **2005,** 38, (7), 2606.

[15] Yang, Y.; Xie, X.; Wu, J.; Yang, Z.; Wang, X.; Mai, Y.-W. *Macromol. Rapid Commun.* **2006,** 27, 1695.

[16] Campidelli, S.; Sooambar,C.; Diz,E.L.; Ehli, C.; Guldi, D.M.; Prato, M. *J. Am. Chem. Soc.* **2006,** 128, 12544.

[17] Wang, D. H.; Baek, J.-B.; Tan, L.-S. Polym. Sci. Eng. B. 2006, 132 103.

[18] Shu, C.-F.; Leu, C.-M. *Macromolecules* **1999**, *32*, 100.

[19] Smith, K.; Jones, D. *J. Chem. Soc., Perkin Trans. 1* **1992**, (4), 407-8.

[20] Melendez, A.; De la Campa, J. G.; De Abajo, J. *Polymer* **1988,** 29, (6), 1142-5.

[21] Stockel, R. F.; Hall, D. M. *Nature*, **1963**, 197, 787.

[22] Vogler, E. A.; Hayes, J. M. *J. Org. Chem.* **1979,** 44, (21), 3682.

[23] (a) Wang, X.; Liu, H.; Jin, Y.; Chen, C. *J. Phys. Chem. B* **2006,** 110, 10236.; (b) Hill, D.; Lin, Y.; Qu, L.; Kitaygorodskiy, A.; Connell, J.W. Allard, L.F.; Sun, Y.-P. *Macromolecules* **2005**, *38*, 7670. (c) Holzinger, M.; Abraham, J.; Whelan, P.; Graupner, R.; Ley, L.; Hennrich, F.; Kappes, M.; Hirsch, A. *J. Am. Chem. Soc.* **2003,** 125, 8566; (d) Lin, Y.; Rao, A. M.; Sadanadan, B.; Kenik, E. A.; Sun, Y.-P. *J. Phys. Chem. B* **2002,** 106, 1294; (e) Holzinger, M.; Vostrowsky, O.; Hirsch, A.; Hennrich, F.; Kappes, M.; Weiss, R.; Jellen, F. *Angew. Chem., Int. Ed.* **2001,** 40, 4002-4005. (f) Sun, Y.-P.; Huang, W.; Lin, Y.; Fu, K.; Kitaygorodskiy, A.; Riddle, L. A.; Yu, Y. J.; Carroll, D. L. *Chem. Mater.* **2001**, *13*, 2864.

[24] We had observed that besides VGCNF, several MWNT samples containing metal contaminants such as iron showed considerably lower residue in TGA experiments after PPA treatment, indicating that most of metal contaminants had been removed after this treatment.

[25] J.-Y. Choi, S.-J. Oh, H.-J. Lee, D. H, Wang, L.-S. Tan, J.-B. Baek, *Macromolecules* accepted for publication.